Probing the Electronic Band Gap of Solid Hydrogen by Inelastic X-Ray Scattering up to 90 GPa

Bing Li,[1] Yang Ding,[1] Duck Young Kim,[1] Lin Wang,[1,2] Tsu-Chien Weng,[1,3,*] Wenge Yang,[1] Zhenhai Yu,[1] Cheng Ji,[1,4] Junyue Wang,[1] Jinfu Shu,[1] Jiuhua Chen,[5] Ke Yang,[6] Yuming Xiao,[4] Paul Chow,[4] Guoyin Shen,[4] Wendy L. Mao,[7,8] and Ho-Kwang Mao[1,†]

[1]*Center for High Pressure Science and Technology Advanced Research, Shanghai 201203, China*
[2]*Center for High Pressure Science (CHiPS), State Key Laboratory of Metastable Materials Science and Technology, Yanshan University, Qinhuangdao, Hebei 066004, China*
[3]*Stanford Synchrotron Radiation Lightsource, SLAC National Accelerator Laboratory, Menlo Park, California 94025, USA*
[4]*HPCAT, X-ray Science Division, Argonne National Laboratory, Argonne, Illinois 60439, USA*
[5]*Center for the Study of Matter at Extreme Conditions, Department of Mechanical and Materials Engineering, Florida International University, Miami, Florida 33199, USA*
[6]*Shanghai Synchrotron Radiation Facility (SSRF), Shanghai Advanced Research Institute, Chinese Academy of Sciences, Shanghai 201204, China*
[7]*Department of Geological Sciences, Stanford University, Stanford, California 94305, USA*
[8]*Stanford Institute for Materials and Energy Sciences, SLAC National Accelerator Laboratory, Menlo Park, California 94025, USA*

(Received 1 July 2020; revised 7 October 2020; accepted 23 December 2020; published 21 January 2021)

Metallization of hydrogen as a key problem in modern physics is the pressure-induced evolution of the hydrogen electronic band from a wide-gap insulator to a closed gap metal. However, due to its remarkably high energy, the electronic band gap of insulating hydrogen has never before been directly observed under pressure. Using high-brilliance, high-energy synchrotron radiation, we developed an inelastic x-ray probe to yield the hydrogen electronic band information *in situ* under high pressures in a diamond-anvil cell. The dynamic structure factor of hydrogen was measured over a large energy range of 45 eV. The electronic band gap was found to decrease linearly from 10.9 to 6.57 eV, with an 8.6 times densification ($\rho/\rho_0 \sim 8.6$) from zero pressure up to 90 GPa.

DOI: 10.1103/PhysRevLett.126.036402

The deep-rooted interest in "metallization of hydrogen" is in the rich physics displayed by the extraordinary changes of hydrogen band gap from a very wide-gap insulator, to a semiconductor, to a metal over an extensive range of pressures and temperature. The theoretically predicted trend is the pressure-induced delocalization of the hydrogen 1*s* electrons from their diatomic orbitals tightly bounded within individual H_2 molecules to become itinerant [1], resulting in a metal or even a superconductor [2]. While observations of metallic behavior have been the focus in numerous static and dynamic studies of solid [3–6] and liquid hydrogen [7–9], the fundamental physics of the insulator region is far from understood. In fact, the very basic electronic band structure, which includes the valance band, conduction band, and the forbidden energy gap in between, has never been observed directly in hydrogen under pressure. The present report focuses on a direct study of the hydrogen electronic band gap and joint density of state of its insulating phase as a function of pressure up to 90.2 GPa.

Diamond-anvil cell (DAC) is the only available technique capable of compressing hydrogen up to several hundred GPa static pressures. The high-pressure electronic band gap closure of hydrogen has been reported based on electrical conductivity measurements [5] which are suitable for semiconductor with a narrow band gap and metal with a closed gap but provide little information on a wide-gap insulator. Electronic band gaps have also been studied using optical absorption or reflection spectroscopy in the DAC with axial geometry [Fig. 1(a)]. The optical method has the limitation that the probing photons must pass through the diamond anvils. The diamond intrinsic band gap of 8 eV [10] sets the upper limit of optical photon energies within the infrared (IR) to near ultraviolet (NUV) range (0.1–5 eV). The unfilled conduction band of solid molecular hydrogen at 10–50 eV above the ground-state electrons in the valence band greatly exceeds this limit, and requires vacuum ultraviolet (VUV) photons at high energies (6–120 eV) that are completely blocked by the diamond. Consequently, the only direct measurement of hydrogen electronic band structure was obtained on cryogenically condensed solid hydrogen at 2 K under high vacuum ($<10^{-7}$ torr) using synchrotron VUV radiation [11].

All previous studies of the band gap in insulating hydrogen as a function of pressure [6,12–18] were based on an indirect scheme using optical measurements with

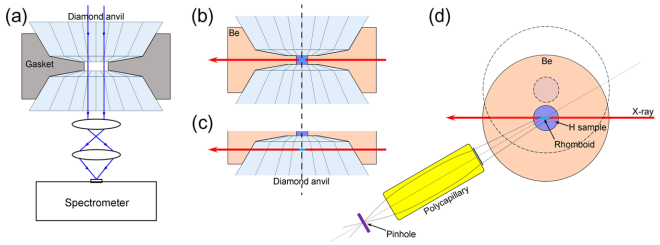

FIG. 1. Schematic drawings showing typical (a) optical and (b)–(d) IXS geometries using a DAC; (a)–(c) side view and (d) top view are not drawn to scale. The red lines in (b) and (d) show the narrowly focused incident x-ray beam passing through the blue hydrogen sample while avoiding the diamond anvils on top and bottom (b), and gasket on the side (d). (c) the diamond anvil was moved 100 μm vertically to collect signal from the diamond background and (d) the dotted line shows the DAC was moved 150 μm sideways to collect the Be gasket background. An x-ray confocal "polycapillary" device is used to select the signal coming from the rhomboid-shaped (light blue colored) portion of the hydrogen sample.

low-energy optical photons passing through the diamond windows [Fig. 1(a)]. This scheme relies on measurements of hydrogen reflectance at the diamond-hydrogen interface as a function of photon frequency $R(\omega)$, which is used to estimate the hydrogen refractive index (n_H) using the Fresnel equation:

$$R(\omega) = (n_D - n_H)^2/(n_D + n_H)^2 . \quad (1)$$

Then n_H as a function of photon frequency is determined at each pressure and used to estimate the plasma frequency that implies band-gap energy of hydrogen. However, a key parameter n_D, the diamond refractive index, is only known at ambient conditions. Not only does n_D change drastically under pressure, but also the change depends upon the differentially strained conditions at the diamond tip that vary from experiment to experiment. The situation is even worse above 200 GPa when the diamond band gap narrows and the diamond windows change color and darken [17,19]. Derivation of hydrogen optical properties from measurements through diamond windows which also undergo their own dramatic changes in optical properties becomes irreproducible. The claims of hydrogen band-gap closure in literature, have therefore been often debated [20–24].

Ideally, inelastic x-ray spectroscopy (IXS) offers a solution for avoiding the interference of diamond and direct study of the high-energy electronic transitions through a nonresonant x-ray Raman scattering process [25,26]. The incident high-energy x ray ($E_0 \sim 10^4$ eV, x ray in) can be used to penetrate the beryllium gasket that forms the pressure chamber of the DAC, to reach the hydrogen sample in the chamber [Figs. 1(b)–1(d)]. The incident x-ray photons transfer a small fraction of their energy $\hbar\omega$, corresponding to the excitation of hydrogen valence band electrons into the conduction band, and then exit the pressure chamber at a slightly reduced energy (E, x-ray out). The excitation energy across the band gap, to any part of the conduction band, is on the order of tens of eV which is 3 orders of magnitude smaller than E_0 or E, and can be measured simply by the difference of the x-ray energies E_0 and E, i.e., the energy transfer,

$$\hbar\omega = E_0\text{-}E . \quad (2)$$

IXS has been used successfully to probe the electronic band structure, excitons, and band gap of a very-wide-gap insulator, the crystalline helium, up to 17 GPa [27]. However, hydrogen presents a greater challenge due to a number of obstacles: (1) IXS is a count-limited technique with very weak x-ray scattering signals from the double differential scattering cross section; (2) as the lightest element, hydrogen is by far the weakest x-ray scatterer. In comparison, all sample-containment materials in the pressure cell, such as Be gasket and diamond anvils, act as heavy elements that produce overwhelming background signals that must be discriminated; (3) high pressures are achieved by minimizing the sample volume, thus further reducing the sample signals. The present efforts in development of DAC IXS have overcome these challenges to accomplish the direct measurement of the electronic band of hydrogen up to 90.2 GPa.

Although the third-generation, high-energy synchrotron sources can provide sufficient brilliance for excitation of the weak hydrogen IXS signals, the intense x-ray beam also generates very strong background signals from the surrounding materials. It is essential to limit the measurement to the microscopic hydrogen sample region, and exclude sampling of the surrounding materials. We conducted the IXS measurements on pressurized hydrogen in DAC in a radial geometry, i.e., both incident and scattered x-ray beam are in the plane normal to the DAC compression axis [Figs. 1(b)–1(d)]. To avoid the background signals from the diamonds and gasket, and maximize the signal-to-background ratio, we focused the incident x-ray beam to a height and width that would keep the beam passing through the hydrogen sample at the center of the gasket hole within the narrow gap between the two diamond anvils [Fig. 1(b)]. The focused incident beam through gasket can completely avoid the top and bottom diamonds and gasket on both sides, but cannot avoid the gasket along the beam before and after the hydrogen sample, which must be discriminated by the signal collection geometry. The scattered beam is collected at a fixed momentum transfer of $q = 4\pi \sin\theta/\lambda$, where $\theta = 15°$ is the scattering angle, and λ is the x-ray wavelength. We used a newly developed x-ray confocal "polycapillary" device [28,29] to focus on the desired beam segment through a confocal pinhole aperture which selects the scattered photons from a rhomboid-shaped portion of hydrogen sample volume and discriminates against the Be

gasket signal along the incident beam upstream and downstream of the rhomboid sample [Fig. 1(d)]. After the pinhole, the scattered x-ray photons proceed to the analyzer crystal that refocuses the x ray at a fixed energy E onto the detector which is on the same Rowland circle with the analyzer and pinhole [25,26]. By scanning the incident beam energy E_0 and collecting energy loss spectra, we were able to observe the electronic band structure of dense solid hydrogen up to 90.2 GPa.

High-pressure IXS experiments were carried out to study the 1s charge excitation of hydrogen. In Fig. 2(a), hydrogen at 6.6 GPa shows the typical behavior of a very-wide-gap insulator with no excitation intensity below 9.37 eV and a very steep rise to a broad peak maximum around 30 eV which include the integrated electron density of states of the conduction band and excitons. The hydrogen sample in the DAC is polycrystalline, and the broad peak represents the joint electron density of states (JDOS) connecting occupied and unoccupied single electron states integrated across the Brillouin zone. The low-energy loss region with zero intensity corresponds to the electron forbidden band gap. The sharp rise at 9.37 eV indicates the threshold of a preedge 1s exciton peak which is experimentally inseparable from the continuum of the conduction band [11]. The continuum above 9.37 eV indicates the sum of excitations of electrons in the valence band to various levels of the conduction band at different Brillouin zone orientations.

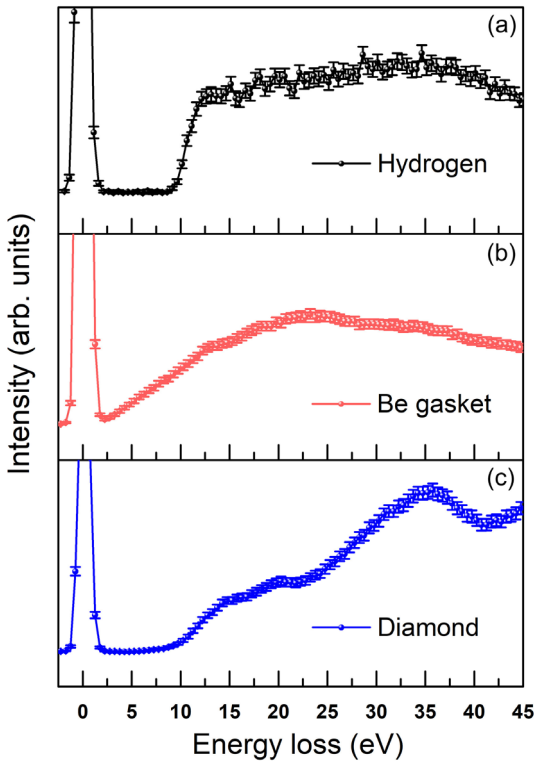

FIG. 2. IXS spectra of (a) solid hydrogen, (b) Be gasket, and (c) diamond anvil at 6.6 GPa. The off-scale peak at zero energy loss is the elastic peak of the incident x ray.

Figures 2(a)–2(c) show the raw data from hydrogen sample, diamond, and the Be gasket without any background subtraction.

Reference spectra from the Be gasket and diamond anvil collected 100–150 μm away from the hydrogen sample are presented for comparison [experiment setup shown in Figs. 1(c) and 1(d) dotted]. The spectra from hydrogen, Be, and diamond in Figs. 2(a)–2(c), respectively, show distinct features. The Be gasket spectrum shows typical metallic behavior without a band gap; its IXS intensity rises immediately from zero energy transfer and increases with energy loss to a maximum at ~20 eV. The diamond-anvil spectrum shows typical insulator behavior with zero intensity at energy loss below the diamond band gap. The diamond excitation begins at ~8 eV, and additional rises were detected at 15–20 and 35–40 eV. Both IXS spectra of Be and diamond match those from literature [10,30]. We compared our measured hydrogen IXS with the distinctive features of Be and diamond control spectra during each measurement to ensure that the background signals were eliminated.

Seven independent hydrogen-in-DAC experiments were conducted at ambient temperature, and twenty-one IXS measurements at various pressures were obtained at synchrotron beamlines 16ID-D of the Advanced Photon Source (APS), Argonne National Laboratory, USA, and 15U1 of Shanghai Synchrotron Radiation Facility (SSRF), China (see Supplemental Material [31] for more details). The IXS measurements were very time demanding. The spectrum for each pressure point in Fig. 3 represents signal integrations of tens of hours. The IXS features of hydrogen evolve continuously with increasing pressure from 6.6 to 90.2 GPa [Fig. 3(a)]: the band gap narrows, the excitation threshold shifts to lower energy loss, the steep slope of the sharp rise above the threshold decreases, and the JDOS broadens, changes shape, with a peak shifting to higher energy. The high-pressure JDOS of solid hydrogen which sums valence-band to conduction-band electron transitions excited by x-ray photons over the entire Brillouin zone, is obtained experimentally for the first time. The broad featureless JDOS lumps together too much information that cannot be delineated at the present time. Nevertheless, it demonstrates direct experimental measurement of high-energy hydrogen conduction band at high pressures, thus opening the exciting perspective for future single-crystal hydrogen electrons IXS studies along Brillouin zone branches to garner detailed information of its band structure.

The only distinctive and well-defined feature of the JDOS is the singular point of threshold energy which defines the hydrogen band gap. As exemplified by the insets of Fig. 3(b), experiments at lower pressures used a larger sample (Supplemental Material [31]) that the IXS signal displayed no intensity within the hydrogen band gap, but at higher pressures, smaller diamond culets and smaller

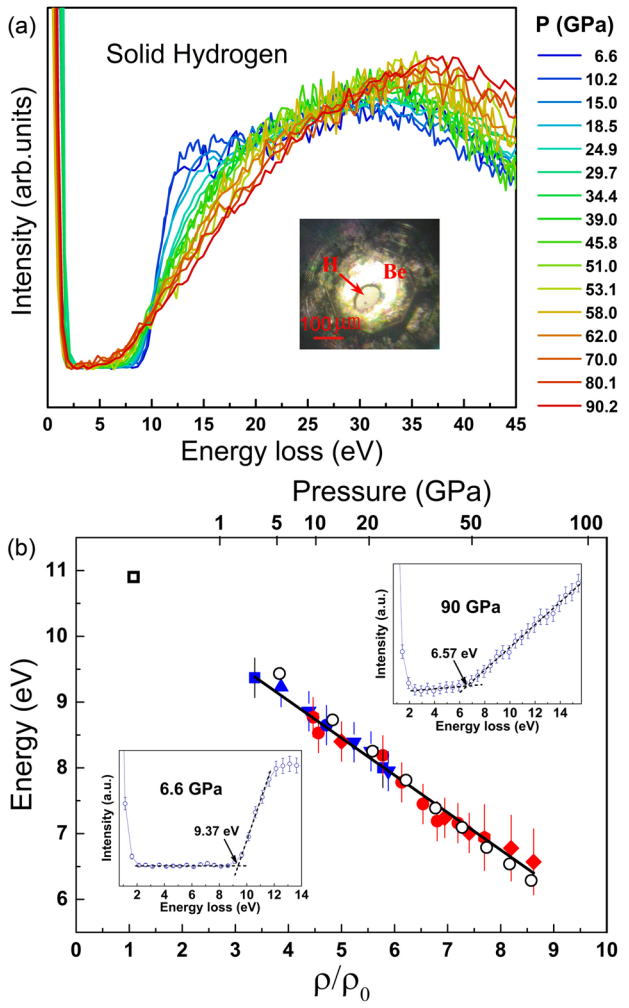

FIG. 3. (a) IXS spectra of solid hydrogen at high pressures from 6.6 to 90.2 GPa. The inset photomicrograph shows the 100 μm hydrogen sample at 90.2 GPa. (b) The band gap of solid hydrogen determined at the breaking points of the slopes of the IXS spectra (illustrated in the insets); blue, experiments at APS; red, experiments at SSRF; seven different solid symbols represent separate DAC IXS experiments; open square, the zero pressure ($<10^{-7}$ torr), low temperature (2 K) threshold energy from Ref. [11]; open circles, theoretical calculations; solid line, linear regression of the IXS experimental data.

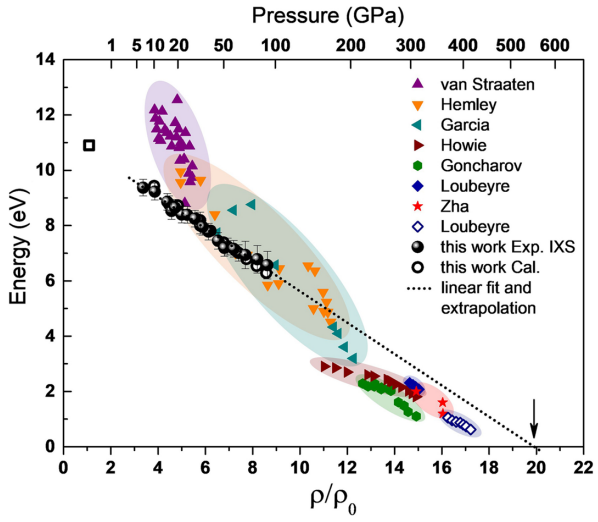

FIG. 4. Threshold energy of solid hydrogen from IXS as a function of density and pressure. The open square corresponds to the zero pressure ($<10^{-7}$ torr), low temperature (2 K) threshold energy from Ref. [11]. Open circles represent the data from theoretical calculations in this work. Filled black circles are IXS data from this work compared with experimental data from Van Straaten [12] (upward triangles), Hemley [13] (downward triangles), Garcia [14] (left triangles), Howie [15] (right triangles), Goncharov [16] (hexagons), Loubeyre [17] (diamonds), Zha [18] (stars), and Loubeyre [6] (open diamonds). The shade areas show the scattering of the data set with the same color hues. The dotted line shows the trend of band-gap closure as a guide for the eye.

sample chambers were used, and the confocal resolution was insufficient to eliminate the Be background completely as shown by the characteristic Be signal of the rising IXS intensity slope immediately from zero energy transfer. The hydrogen threshold energy is thus defined as the intersection point between the Be background slope and the much steeper hydrogen slope.

The hydrogen band gap is plotted as a function of density (and pressure) in Fig. 3(b). The experimental equation of state of hydrogen [32] was used for the pressure-to-density conversion. The 21 data points from seven experiments conducted at two synchrotron facilities (APS and SSRF) over a four-year period covering the range from 9.37 eV at 6.6 GPa to 6.57 eV at 90.2 GPa are in very good agreement. The results show an empirical linear relationship between band-gap energy (E_g) and density within this pressure range:

$$E_g(\mathrm{eV}) = 11.3(1) - 0.57(2)(\rho/\rho_0)\,. \tag{3}$$

The experimental data are in excellent agreement with our band-gap calculations (Fig. 4). To calculate quantitatively accurate band gaps, we used Heyn-Scuseria-Ernzerhof (HSE)-type hybrid functional within the density functional theory. In a recent benchmark, HSE was found to better describe solid hydrogen behavior at extreme conditions such as insulator-to-metal and liquid-to-liquid transitions over other semilocal functionals referenced by a quantum Monte Carlo result [33] (see Supplemental Material [31] for detailed information about computational structure relaxation and band-gap estimation, which includes Refs. [34–40] and [41–46], respectively.)

E_g is the key parameter that many previous studies on the hydrogen metallization process have pursued using the optical scheme of Eq. (1) [6,12–18] and extrapolations of the data in insulator or semiconductor regions to estimate the band-gap closure points. As shown in Fig. 4, the actual data of each individual study covered a cluster of data points with very large scattering. Their linear extrapolations

predicted band-gap closure pressure varying with a huge uncertainty of 101 to 652 GPa. The present data from IXS, on the other hand, present a very tight constraint of the band-gap variation in the wide-gap insulator region up to 90.2 GPa. Linear extrapolation of the decreasing band gap, albeit a rough estimation, would reach a closure density ratio (ρ/ρ_0) of 19.9 which corresponds to ~550 GPa with uncertainty of ~35 GPa. It should be noted that the extrapolation is applicable only for the same phase with the same crystal structure. At least four phase transitions have been reported above 150 GPa based on changes in optical Raman and IR spectroscopy, but x-ray diffraction studies indicate that the hydrogen remains in the hexagonal close-packed structure with continuous ρ/ρ_0 as a function of pressure in phases III and IV [47]. Therefore, although the main purpose of the present IXS study remains on accurate characterization of the insulator phase, its extrapolation also serves as a guideline for the effects of hydrogen phase transitions on metallization, as well as a comprehensive comparison of previous studies and data over the extensive range of compression.

In summary, we have demonstrated the use of IXS as a selective and penetrating probe for collecting electronic band structure information on dense hydrogen in the previously inaccessible VUV energy range, including how the electronic JDOS and band gap evolve with pressure. We obtained precise constraints on the band gap as a function of density in the insulator region up to 90 GPa. Taking advantage of the developments in state-of-the-art synchrotron capabilities with submicron to nanometer-scaled x-ray probes, future advances of IXS to higher pressures may reach the semiconductor region of phases II–V, and may enable the study of hydrogen metallization based on direct and quantitative electronic band-gap measurements rather than relying on the result of the extrapolation. Ultimately it opens the possibility to select orientated single crystals of hydrogen [47] to resolve the dispersions along different Brillouin zone branches [10,30], thus garnering true understanding of the solid hydrogen electronic band structure under compression.

This research was supported by NSFC Grants No. U1530402 and No. U1930401. D. Y. K. acknowledges the support from NSFC-11774015 and J. C. acknowledges the support from NSF (EAR-1723185). Technical assistance from 15U1 at SSRF is gratefully acknowledged. Portions of this work were performed at HPCAT (Sector 16), which is supported by DOE-BES under Award No. DE-FG02-99ER45775. HPCAT operations are supported by DOE-NNSA's Office of Experimental Sciences. This research used resources of the Advanced Photon Source, a U.S. DOE Office of Science User Facility operated for the DOE Office of Science by Argonne National Laboratory under Contract No. DE-AC02-06CH11357.

*Present address: School of Physical Science and Technology, ShanghaiTech University, Shanghai 201210, China.
†maohk@hpstar.ac.cn

[1] E. Wigner and H. B. Huntington, J. Chem. Phys. **3**, 764 (1935).
[2] N. W. Ashcroft, Phys. Rev. Lett. **21**, 1748 (1968).
[3] H. K. Mao and R. J. Hemley, Science **244**, 1462 (1989).
[4] R. P. Dias and I. F. Silvera, Science **355**, 715 (2017).
[5] M. I. Eremets, A. P. Drozdov, P. P. Kong, and H. Wang, Nat. Phys. **15**, 1246 (2019).
[6] P. Loubeyre, F. Occelli, and P. Dumas, Nature (London) **577**, 631 (2020).
[7] W. J. Nellis, S. T. Weir, and A. C. Mitchell, Science **273**, 936 (1996).
[8] M. D. Knudson, M. P. Desjarlais, A. Becker, R. W. Lemke, K. R. Cochrane, M. E. Savage, D. E. Bliss, T. R. Mattsson, and R. Redmer, Science **348**, 1455 (2015).
[9] P. M. Celliers *et al.*, Science **361**, 677 (2018).
[10] W. A. Caliebe, J. A. Soininen, E. L. Shirley, C. C. Kao, and K. Hämäläinen, Phys. Rev. Lett. **84**, 3907 (2000).
[11] K. Inoue, H. Kanzaki, and S. Suga, Solid State Commun. **30**, 627 (1979).
[12] J. van Straaten and I. F. Silvera, Phys. Rev. B **37**, 6478 (1988).
[13] R. J. Hemley, M. Hanfland, and H. K. Mao, Nature (London) **350**, 488 (1991).
[14] A. García, M. L. Cohen, J. H. Eggert, F. Moshary, W. J. Evans, K. A. Goettel, and I. F. Silvera, Phys. Rev. B **45**, 9709 (1992).
[15] R. T. Howie, C. L. Guillaume, T. Scheler, A. F. Goncharov, and E. Gregoryanz, Phys. Rev. Lett. **108**, 125501 (2012).
[16] A. F. Goncharov, J. S. Tse, H. Wang, J. Yang, V. V. Struzhkin, R. T. Howie, and E. Gregoryanz, Phys. Rev. B **87**, 024101 (2013).
[17] P. Loubeyre, F. Occelli, and R. LeToullec, Nature (London) **416**, 613 (2002).
[18] C.-S. Zha, Z. Liu, and R. J. Hemley, Phys. Rev. Lett. **108**, 146402 (2012).
[19] H. K. Mao and R. J. Hemley, Nature (London) **351**, 721 (1991).
[20] A. F. Goncharov and V. V. Struzhkin, Science **357**, eaam9736 (2017).
[21] X.-D. Liu, P. Dalladay-Simpson, R. T. Howie, B. Li, and E. Gregoryanz, Science **357**, eaan2286 (2017).
[22] I. Silvera and R. Dias, Science **357**, eaan1215 (2017).
[23] D. Castelvecchi, Nature (London) **542**, 17 (2017).
[24] E. Gregoryanz, C. Ji, P. Dalladay-Simpson, B. Li, R. T. Howie, and H.-K. Mao, Matter Radiat. Extremes **5**, 038101 (2020).
[25] J.-P. Rueff and A. Shukla, Rev. Mod. Phys. **82**, 847 (2010).
[26] G. Shen and H. K. Mao, Rep. Prog. Phys. **80**, 016101 (2017).
[27] H. K. Mao *et al.*, Phys. Rev. Lett. **105**, 186404 (2010).
[28] P. Chow, Y. M. Xiao, E. Rod, L. G. Bai, G. Y. Shen, S. Sinogeikin, N. Gao, Y. Ding, and H.-K. Mao, Rev. Sci. Instrum. **86**, 072203 (2015).
[29] C. A. MacDonald, X-Ray Opt. Instrum. **2010**, 867049 (2010).

[30] W. Schülke, H. Nagasawa, S. Mourikis, and A. Kaprolat, Phys. Rev. B **40**, 12215 (1989).
[31] See Supplemental Material at http://link.aps.org/supplemental/10.1103/PhysRevLett.126.036402 for further details concerning the experiments and theoretical calculations.
[32] P. Loubeyre, R. LeToullec, D. Hausermann, M. Hanfland, R. J. Hemley, H. K. Mao, and L. W. Finger, Nature (London) **383**, 702 (1996).
[33] R. C. Clay III, J. Mcminis, J. M. McMahon, C. Pierleoni, D. M. Ceperley, and M. A. Morales, Phys. Rev. B **89**, 184106 (2014).
[34] G. Kresse and J. Furthmüller, Comput. Mater. Sci. **6**, 15 (1996).
[35] P. Hohenberg and W. Kohn, Phys. Rev. **136**, B864 (1964).
[36] W. Kohn and L. J. Sham, Phys. Rev. **140**, A1133 (1965).
[37] J. P. Perdew, J. A. Chevary, S. H. Vosko, K. A. Jackson, M. R. Pederson, D. J. Singh, and C. Fiolhais, Phys. Rev. B **46**, 6671 (1992).
[38] J. P. Perdew, K. Burke, and M. Ernzerhof, Phys. Rev. Lett. **77**, 3865 (1996).
[39] C. J. Pickard and R. J. Needs, Nat. Phys. **3**, 473 (2007).
[40] S. Azadi and W. M. C. Foulkes, Phys. Rev. B **88**, 014115 (2013).
[41] A. V. Krukau, O. A. Vydrov, A. F. Izmaylov, and G. E. Scuseria, J. Chem. Phys. **125**, 224106 (2006).
[42] J. Heyd, G. E. Scuseria, and M. Ernzerhof, J. Chem. Phys. **118**, 8207 (2003).
[43] L. Monacelli, I. Errea, M. Calandra, and F. Mauri, Nat. Phys. **17**, 63 (2021).
[44] V. Gorelov, M. Holzmann, D. M. Ceperley, and C. Pierleoni, Phys. Rev. Lett. **124**, 116401 (2020).
[45] M. A. Morales, J. M. McMahon, C. Pierleoni, and D. M. Ceperley, Phys. Rev. Lett. **110**, 065702 (2013).
[46] M. Stadele and R. M. Martin, Phys. Rev. Lett. **84**, 6070 (2000).
[47] C. Ji *et al.*, Matter Radiat. Extremes **5**, 038401 (2020).